



Enantioselective degradation and bioaccumulation of sediment-associated fipronil in *Lumbricus variegatus*: Toxicokinetic analysis

Shunhui Wang^{a,b,c,d}, Huizhen Li^b, Jing You^{b,*}

^a State Key Laboratory of Organic Geochemistry, Guangzhou Institute of Geochemistry, Chinese Academy of Sciences, 510640 Guangzhou, China

^b School of Environment and Guangdong Key Laboratory of Environmental Pollution and Health, Jinan University, 510632 Guangzhou, China

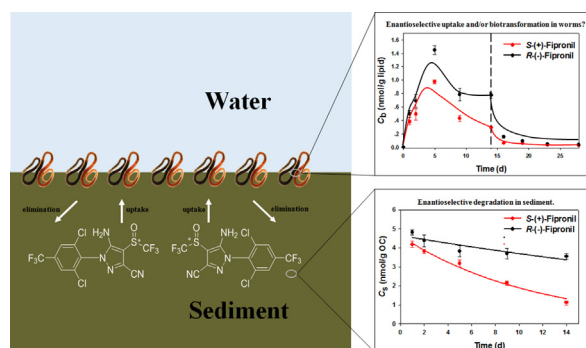
^c School of Chemistry and Chemical Engineering, Oil & Gas Field Applied Chemistry Key Laboratory of Sichuan Province, Southwest Petroleum University, Chengdu 610500, China

^d University of Chinese Academy of Sciences, Beijing 100049, China

HIGHLIGHTS

- Faster degradation of *S*-(+)-fipronil resulted in higher *R*-(-)-fipronil levels in sediment.
- Bioaccumulation of sediment-bound fipronil to *L. variegatus* was enantioselective.
- Biotransformation of *R*-(-)-fipronil was faster than *S*-(+)-fipronil in *L. variegatus*.
- Preferential uptake of *R*-(-)-fipronil was the main reason for its higher body residues.
- Toxicokinetic modeling explained the bioaccumulation process of chiral pesticide.

GRAPHICAL ABSTRACT



ARTICLE INFO

Article history:

Received 5 February 2019

Received in revised form 26 March 2019

Accepted 31 March 2019

Available online 1 April 2019

Editor: Jay Gan

Keywords:

Toxicokinetic modeling

Enantioselective degradation

Enantioselective biotransformation

Benthic invertebrates

Chiral pesticide

ABSTRACT

Enantioselective degradation and biotransformation are critical processes affecting the bioaccumulation and toxicity of chiral pesticides in the environment. In the present study, enantioselective uptake, biotransformation and elimination of a current use pesticide, fipronil in a benthic invertebrate, *Lumbricus variegatus* were assessed using a sediment bioaccumulation test. Toxicokinetic models were constructed to quantitatively describe kinetic processes of fipronil enantiomers. The degradation of fipronil in sediment significantly affected chemical uptake, thus degradation kinetic model was incorporated into toxicokinetic modeling. It was shown that *S*-(+)-fipronil degraded faster than *R*-(-)-fipronil in sediment, with dissipation rate constants being 0.090 ± 0.008 and 0.023 ± 0.006 1/d, respectively. As a result, *R*-(-)-enantiomer preferentially accumulated in sediment over time. Similarly, higher concentrations of *R*-(-)-fipronil were detected in *L. variegatus* compared with *S*-(+)-fipronil. Toxicokinetic modeling showed *R*-(-)-fipronil had larger uptake and elimination rate coefficients and apparent maximum reaction rate, but a smaller apparent half-saturation constant than *S*-(+)-fipronil. Preferential uptake of *R*-(-)-fipronil from sediment to *L. variegatus* was the main reason for greater *R*-(-)-fipronil concentrations in organism. Biotransformation of fipronil in *L. variegatus* was also enantioselective, yet it played fewer roles on enantioselective bioaccumulation than uptake. Overall, our findings highlight the importance of selective degradation, uptake and biotransformation of sediment-associated fipronil on its enantioselective bioaccumulation in benthic invertebrates, which helps to improve the accuracy for assessing aquatic toxicity of the chiral pesticide.

* Corresponding author.

E-mail address: youjing@jnu.edu.cn (J. You).

Capsule: Enantioselective bioaccumulation of sediment-associated fipronil in *Lumbricus variegatus* was quantitatively explained by selective degradation, uptake, biotransformation and elimination parameters using a combination of degradation and toxicokinetic modeling.

© 2019 Elsevier B.V. All rights reserved.

1. Introduction

Chirality is defined as any geometric configuration that cannot completely overlap its image. Approximately a quarter of pesticides in the global marketplace contain chiral centers and the portion is still growing (Xu et al., 2018). Although it is well documented that biological effects of stereoisomers may be greatly different, most chiral pesticides on sale are applied as racemate (Liu et al., 2005; Qian et al., 2017). In addition to disparate toxicodynamic (TD) interactions with biological receptors between enantiomers, toxicokinetic (TK) variations between enantiomers also play an important role in enantioselective toxicity as TK processes directly determine internal doses of pesticides in the organisms (Cantillana, 2009; Qu et al., 2016a).

Toxicokinetic processes describe absorption, distribution, metabolism and elimination (ADME) of a chemical in biota versus exposure time course (Ashauer and Escher, 2010). Modeling TK process helps to elucidate the fate of a chemical in vivo and to improve the accuracy of predicting toxicological outcomes of xenobiotics to individual organisms and populations which are of regulatory importance (Ashauer and Jager, 2018; Li et al., 2018). The TK modeling has also been utilized to extrapolate toxicity assessment across species which share similar physiological traits or habitat (Wiberg-Larsen et al., 2016). The ADME parameters from TK models are beneficial in identifying key processes associated with bioaccumulation of enantiomers and providing information to study enantioselective toxicity mechanistically.

Compared with legacy organochlorine pesticides, current-use pesticides have a greater tendency to be transformed in biota and abiotic environment, requiring better understanding on the roles of degradation and biotransformation on the bioaccumulation of the pesticides. For example, fipronil transformed to fipronil sulfone and highly polar conjugates in corn rootworm, to fipronil sulfone in tilapia, and to fipronil desulfinyl, fipronil sulfone and fipronil sulfide in *Lemna minor*-sediment-*Anodonta woodiana* ecosystems (Li et al., 2018; Qu et al., 2016a; Scharf et al., 2000). As a result of its extensive use, fipronil was widely detected in sediment along with its degradation products and was regarded as one of the key stressors responsible for sediment toxicity to benthic organisms in the U.S. and in China (Wei et al., 2017; Weston and Lydy, 2014). Fipronil is a chiral insecticide and its enantioselective bioaccumulation varied across species, e.g., more *R*-(−)-fipronil accumulated in *Tubifex tubifex* than *S*-(+)-fipronil (Liu et al., 2012), conversely, more *S*-(+)-fipronil bioaccumulated than *R*-(−)-fipronil in *A. woodiana* (Qu et al., 2016b). As shown in Table S1 (“S” represents the tables and figures in the Supplementary Data thereafter), enantiomer ratios (ERs, *S*-(+)- to *R*-(−)-enantiomer) of fipronil toxicity to most invertebrate species were significantly deviated from 1, suggesting that the toxicity of *S*-(+)- and *R*-(−)-fipronil was different in most cases. For example, the ERs of fipronil toxicity were 0.193 and 1.74 for *A. woodianas* and *Eisenia foetida*, respectively (Qu et al., 2014, 2016b). The TK processes of a chemical in organism were generally controlled by stereospecific enzymatic processes and/or receptors (Hegeman and Laane, 2002; Li et al., 2018), thus enantioselective ADME processes of fipronil enantiomers in biota might partially explain the observed enantioselective toxicity. Furthermore, enantioselective degradation of fipronil in abiotic environment was also observed, e.g., *S*-(+)-fipronil showed greater tendency to be degraded than *R*-(−)-fipronil under anaerobic or acidic/neutral conditions, while *R*-(−)-fipronil had a higher degradation rate under alkaline conditions (Jones et al., 2007; Nillos et al., 2009). Thus, the degradation of fipronil

in the environment should not be ignored when assessing the enantioselective bioaccumulation and toxicity.

The primary goal of the present study was to understand the enantioselective bioaccumulation process of sediment-bound fipronil in a benthic invertebrate, *Lumbricus variegatus*. To achieve the goal, a toxicokinetic model was constructed to determine the parameters related to uptake, biotransformation and elimination processes for individual enantiomers in the blackworms, and to quantitatively elucidate the enantioselective bioaccumulation process. In addition, enantioselective degradation of fipronil in sediment was included to improve the accuracy of toxicokinetic modeling.

2. Materials and methods

2.1. Chemicals and reagents

Neat compounds of fipronil and its main degradation products, fipronil sulfone, fipronil sulfide and fipronil desulfinyl, with purity >98% were purchased from Dr. Ehrenstorfer GmbH (Augsburg, Germany). The internal standard for instrumental analysis, ¹³C-fipronil was bought from Toronto Research Chemicals Incorporation (Ontario, Canada). In addition, 4,4'-dibromooctafluorobiphenyl (DBOBF) and 2,3,3',4,4',5',6-heptachlorobiphenyl (CB-191), which were used as the surrogates to check the efficiency of sample preparation procedures, were purchased from Supelco (Bellefonte, PA, USA) and AccuStandard (New Haven, CT, USA), respectively.

High performance liquid chromatography (HPLC) grade hexane, dichloromethane and 2-propanol were purchased from Oceanpak Alexative Chemical Limited (Gothenburg, Sweden). Analytical grade acetone was obtained from Tianjin Chemical Reagent Factory (Tianjin, China) and redistilled before use. Gel permeation chromatography (GPC) column packed with S-X3 beads (200–400 mesh, Bio-Rad, Hercules, CA, USA) was used for purifying tissue samples. Anhydrous Na₂SO₄ (Tianjin Chemical Reagent Factory) was baked at 450 °C for 4 h before use. Granular carbon black (GCB) and primary/secondary amine (PSA) sorbents were purchased from Agela Technologies (Tianjin, China).

2.2. Sediment collection and spiking

A sediment was collected from a drinking water reservoir in Conghua, China in 2016 and used as control sediment. This sediment was free of toxicity to benthic organisms and contained no fipronil or its degradation products as suggested in the preliminary tests. Total organic carbon (OC) in sediment was quantified using a Vario EL III Elemental Analyzer (Hanau, Germany) after inorganic carbonates being removed with 10% HCl. The control sediment had a Total OC of 1.85 ± 0.14% and a moisture content of 51.3 ± 0.2%.

The sediment was spiked with appropriate amounts of fipronil using acetone as a carrier at a concentration of 100 µL per kg sediment. Fipronil was spiked into the sediment with a nominal concentration being 12.4 nmol/g OC (100 ng/g dry weight). After spiking, the sediment was thoroughly homogenized for 4 h using an overhead stirrer. Spiked sediment was aged at 4 °C in the dark for 28 d and homogenized again before use.

2.3. Bioaccumulation testing

For contact with sediment and ease of laboratory culture, *L. variegatus* has been recommended as a model species for sediment

bioaccumulation tests (USEPA, 2000). The blackworms were cultured at Jinan University, China in accordance with the standard protocols (USEPA, 2000). Bioaccumulation testing was conducted in triplicate in 400-mL beakers containing 80 g of wet sediment and 300 mL of overlying reconstituted water following a previously developed method (Li et al., 2014). In brief, the sediment was allowed to settle overnight, and 30 blackworms were randomly placed into each beaker. The bioassays were carried out at 23 ± 1 °C with a 16:8 light: dark photoperiod. The organisms were not fed throughout the 28-d testing, and approximately 200 mL of overlying water was renewed twice daily using an automated water-delivery system (Mehler et al., 2018). Water quality parameters including pH, temperature, conductivity and dissolved oxygen were monitored daily, and concentrations of ammonia were analyzed every three days.

The bioaccumulation experiment consisted of a 14-d uptake phase and a 14-d elimination phase. Three replicates of exposed organisms were randomly sampled at predetermined time intervals at 1, 2, 5, 9 and 14 d of the uptake phase. At the end of 14-d uptake phase, the organisms from the remaining replicates were sieved from fipronil-spiked sediment and transferred into control sediment to initiate the elimination phase. Three replicates were sampled per time point over the course of the elimination phase, with sampling time points at 16, 19, 23 and 28 d of the bioaccumulation testing (i.e., 2, 5, 9 and 14 d of the elimination phase). At each sampling time, the blackworms were sieved from the sediment, transferred to the beakers containing 300 mL of clean reconstituted water. After 6 h of gut purging, the blackworms were collected from the water, weighed and frozen at -20 °C until chemical analysis. Concurrently, the bioaccumulation testing was also conducted using control sediment and sampling time points were the same as the spiked sediment.

2.4. Chemical analysis

2.4.1. Sediment and biota extraction and cleanup

The concentrations of fipronil and its degradation products in sediment were analyzed in triplicate at each sampling time during the uptake phase. Sample preparation procedures followed a previously developed method (Brennan et al., 2009). Two surrogates, DBOFB and CB-191, were added to each sample before extraction. Approximately 3 g of freeze-dried sediment was extracted with a mixture of acetone and dichloromethane (1:1, v:v) on a Dionex 350 accelerated solvent extractor (ASE, Thermo Scientific, USA). After solvent exchanged to hexane, the extracts were cleaned with solid phase extraction cartridges packed with 600 mg of PSA, 600 mg of GCB and 1 cm of anhydrous Na_2SO_4 from the bottom to the top. The analytes were eluted from the cartridge with 7 mL of dichloromethane and hexane (3:7, v:v) and 7 mL of acetone and hexane (1:1, v:v), sequentially. The effluents were combined, solvent exchanged to hexane, concentrated to 1 mL, and 50 ng of ^{13}C -fipronil was added to the extracts as the internal standard before instrumental analysis.

The concentrations of fipronil and its metabolites in *L. variegatus* were also analyzed. After adding the surrogates, weighed organisms were sonicated with 1.5 mL of a mixture of acetone and hexane (1:1, v:v), and the extraction was repeated twice. The extracts were combined, solvent exchanged to 1 mL of hexane, dried with anhydrous Na_2SO_4 , and purified with the GPC column. The analytes were eluted out of the columns using 14 mL of a mixture of dichloromethane and hexane (1:1, v:v). The extracts were then concentrated, and solvent exchanged to 100 μL of hexane before adding 5 ng of ^{13}C -fipronil as the internal standard.

2.4.2. Instrumental analysis

The concentrations of the surrogates (DBOFB and CB-191), *rac*-fipronil and the degradation products (fipronil sulfide, fipronil sulfone and fipronil desulfinyl) were quantified using a Shimadzu QP-2010-plus series GC/MS (Shimadzu, Japan). Detailed GC/MS conditions are

provided in the Supplementary data. Fipronil enantiomers were analyzed on an AB SCIEX Triple Quad 5500 HPLC/MS/MS installed with a (R,R)-Whelk-O1 chiral column (250 mm \times 4.6 mm i.d., Regis Technologies Incorporation, Morton Grove, IL, USA). A mixture of 2-propanol and hexane (1:9, v:v) was used as the mobile phase and the flow rate was set at 1.6 mL/min. The separation was performed at column temperature of 23 °C with an injection volume of 14 μL . The MS was operated using atmospheric chemical ionization (APCI) in negative ion mode. The desolvation temperature was set at 550 °C and ion spray voltage was -4500 V. The pressures of curtain gas, collision gas and ion source gas were set at 55, 8 and 60 psi, respectively. Multiple reaction monitoring (MRM) was applied for compound qualification and the transition m/z Q1: 435 to Q3: 330, 339 was used for fipronil and m/z Q1: 439 to Q3: 322, 334 for ^{13}C -fipronil. Quantification of analytes was conducted using internal calibration standards at concentrations from 0.1 to 50 ng/mL.

2.4.3. Quality assurance and quality control

A calibration standard was analyzed every 10 samples to ensure instrumental performance, and variations in all check standards were within 20%. A set of quality control samples, including a method blank (solvent), a matrix blank (clean sediment or tissue), a matrix spike and a matrix spike duplicate were concurrently analyzed with every 20 samples. No fipronil or its degradation products were detected in the blanks. Two surrogates (DBOFB and CB-191) were added to all samples before extraction and their recoveries were $86 \pm 17\%$ and $105 \pm 22\%$, respectively. Recoveries for *S*-(+)- and *R*-(-)-fipronil in spiked samples were $90 \pm 4\%$ and $87 \pm 2\%$ in sediment, respectively, and $95 \pm 6\%$ and $89 \pm 4\%$ in organism samples, respectively. The reporting limits for fipronil, which were calculated by dividing the product of the lowest concentration of calibration standards and the extract volume by the sample mass used for extraction, were 0.04 ng/g dw and 0.03 ng/g wet weight (ww) in sediment and biota, respectively.

2.5. Data and statistical analysis

To profile the enantioselective degradation/dissipation process of fipronil during the bioaccumulation testing, the change of sediment concentrations of fipronil enantiomer over time was modeled using a first-order kinetic model (Eq. (1)) (Ding et al., 2012).

$$C_s = C_0 \times e^{-\lambda \times t} \quad (1)$$

where C_s (nmol/g OC) and C_0 are concentrations of *S*-(+)- and *R*-(-)-fipronil in sediment at time t (d) and at the beginning of the exposure, respectively, and λ is the apparent dissipation rate constant. Half-life of the enantiomer in sediment ($t_{1/2, \text{sed}}$) was then calculated from λ using Eq. (2).

$$t_{1/2, \text{sed}} = \ln 2 / \lambda \quad (2)$$

To quantitatively describe enantioselective TK process in the organisms, a simulated procedure was used to estimate the uptake, metabolism and clearance parameters of fipronil enantiomers in *L. variegatus* using the following equations (Landrum et al., 1992).

$$dC_p/dt = k_u \times C_s - k_m \times C_p - k_{ep} \times C_p \quad (3)$$

$$k_m = V_m / (K_s + C_p) \quad (4)$$

where C_p (nmol/g lipid) and C_s (nmol/g OC) represent the concentrations of fipronil enantiomer in biota and sediment, respectively. The k_u (g OC/g lipid/d) is the uptake rate coefficient from sediment to biota for fipronil enantiomer and k_{ep} (1/d) is the elimination rate coefficient for the enantiomer. k_m (1/d) is the biotransformation rate coefficient for fipronil enantiomer in *L. variegatus* and it is estimated from the

apparent half-saturation constant (K_s , nmol/g lipid) and the apparent maximum reaction rate (V_m , nmol/g lipid/d) following the non-linear Michaelis-Menten kinetic model (Eq. (4)).

SigmaPlot 10.0 was used to simulate degradation kinetics for fipronil enantiomers using Eq. (1), and Scientists 2.01 was used to simulate TK process using Eqs. (3) and (4). To take sediment degradation into account when modeling TK process in the organism-sediment system, C_s modeled from Eq. (1) was incorporated into the simulation using Eq. (3). In the present study, the initial analog value of V_m was firstly set as 0.35 and 0.58 for *S*-(+)- and *R*-(-)-fipronil, respectively, and these initial values were estimated from the elimination rate constants in a study on the bioaccumulation of fipronil in *E. foetida* (Qin et al., 2015). The initial values of V_m were estimated by multiplying literature derived elimination rate constants to the concentrations of *S*-(+)- and *R*-(-)-fipronil at 5 d, which reached apex in bioaccumulation testing.

An enantiomer fraction (EF) was used to quantify the enantioselectivity and it was calculated by dividing the concentration of *S*-(+)-enantiomer to the sum of *S*-(+)- and *R*-(-)-enantiomers (Konwick et al., 2006). Statistical differences among chemical concentrations were compared using one-way analysis of variance (ANOVA) followed by Tukey's honestly significant difference testing with SPSS (version 21, IBM, New York, USA). Significant difference was set at $p < 0.05$.

3. Results and discussion

3.1. Enantioselective degradation of fipronil in sediment

Both fipronil enantiomers were detected in the sediment spiked with *rac*-fipronil at a nominal concentration of 12.4 nmol/g OC. As shown in Table S2, the measured concentrations of *S*-(+)- and *R*-(-)-fipronil were 5.97 ± 0.04 and 6.42 ± 0.06 nmol/g OC, respectively, in the freshly spiked sediment. After aging for 28 d at 4 °C, no significant reduction of fipronil concentrations was noted in sediment, being 5.70 ± 0.19 and 6.32 ± 0.11 nmol/g OC for *S*-(+)- and *R*-(-)-fipronil, respectively. On the contrary, fipronil degraded considerably during the 14-d uptake phase of TK tests, and the concentrations dropped to 1.11 ± 0.11 and 3.54 ± 0.16 nmol/g OC at the end of uptake phase for *S*-(+)- and *R*-(-)-fipronil, respectively. Fipronil sulfide ($0-1.20 \pm 0.04$ nmol/g OC) and fipronil sulfone ($0-0.64 \pm 0.01$ nmol/g OC) were the main degradation products detected in the sediment, yet no fipronil desulfinyl was detected. Accelerated dissipation of fipronil during bioaccumulation testing is reasonable. High temperature and moisture contents were favorable for chemical degradation (Kumar et al., 2017; Lewis et al., 1999). While sediment aging was at 4 °C, the bioaccumulation testing was conducted at 23 °C. In addition, renewals of overlying water daily and bioturbation increased moisture content of test sediments.

In addition to the loss of fipronil in sediment, decreasing EF values (*S* to *S* + *R*) for sediment-bound fipronil over time suggested that *S*-(+)-fipronil degraded faster than *R*-(-)-fipronil (Fig. 1 and Table S2). The EF of a racemate for commercial use is close to 0.5, yet EF might change in enantioselective processes. As such, EF has been commonly used to describe enantioselective degradation and biotransformation processes (Konwick et al., 2006). Stereoselective degradation occurred during the 14-d TK uptake phase (23 °C) (change of EF: 0.223 ± 0.014), while the change of EF was negligible in the 28-d aging period (4 °C) (0.008 ± 0.011). Enantioselective degradation of fipronil in sediment over the 14-d uptake phase was modeled following Eq. (1) (Fig. 2). The simulated dissipation rate constants (λ) for *R*-(-)- and *S*-(+)-fipronil were 0.023 ± 0.006 and 0.090 ± 0.008 1/d, respectively. Significantly different λ values for the two enantiomers quantitatively confirmed the preferential degradation of *S*-(+)- fipronil compared with *R*-(-)-fipronil in sediment.

Enantioselective degradation of fipronil has also been documented in previous studies. It has been shown that *S*-(+)-fipronil was less

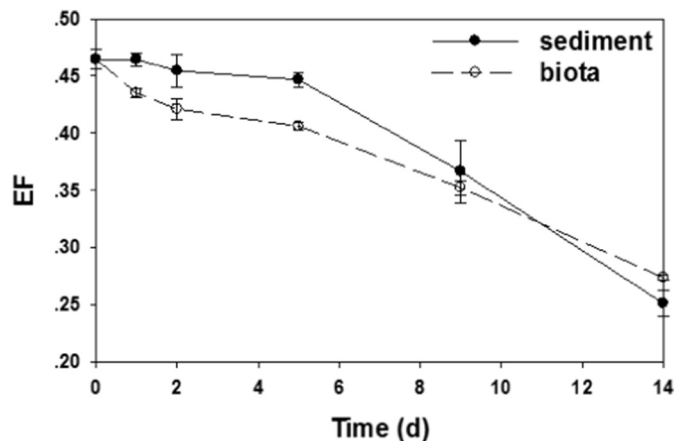


Fig. 1. Enantiomeric fraction of fipronil enantiomers in sediment (solid circle and real line) and biota (hollow circle and dashed line) during the 14-d uptake phase. The EF was the ratio of the concentrations of the *S*-(+)-enantiomer to the sum of *S*-(+)- and *R*-(-)-enantiomers at each time. Error bars represent standard deviations of three replicates.

stable with higher degradation rate for *S*-(+)- than *R*-(-)-fipronil in flooded paddy soil and sediment under anaerobic conditions (Nillos et al., 2009; Tan et al., 2008). This was in accordance with the finding in the present study. Reductive product fipronil sulfide was found to be the dominant degradation product, implying anaerobic condition in the sediment. Half-lives of the two enantiomers in sediment were 7.7 ± 0.7 and 30.1 ± 7.9 d for *S*-(+)- and *R*-(-)-fipronil, respectively. This is similar to a previous study which reported a half-life of 8 d for *S*-(+)-enantiomer and 15 d for the *R*-(-)-isomer in soil (Tan et al., 2008). On the other hand, Jones et al. (2007) did not observe stereoselective degradation of fipronil in sediment with a half-life of *rac*-fipronil of 35–40 d. Different microbial populations or enzymatic systems were regarded as the likely reasons for disparate degradation selectivity of fipronil in various environmental media (Tan et al., 2008).

Overall, fipronil enantiomers selectively degraded in sediment over time, particularly under room temperature and with high moisture in the course of the bioaccumulation testing, and degradation rate of *S*-(+)-fipronil was significantly higher than that of *R*-(-)-fipronil. As a consequence, there was significantly greater amount of *R*-(-)-fipronil residues in sediment. The EF values of sediment-bound fipronil were <0.5 and continuously decreased over time.

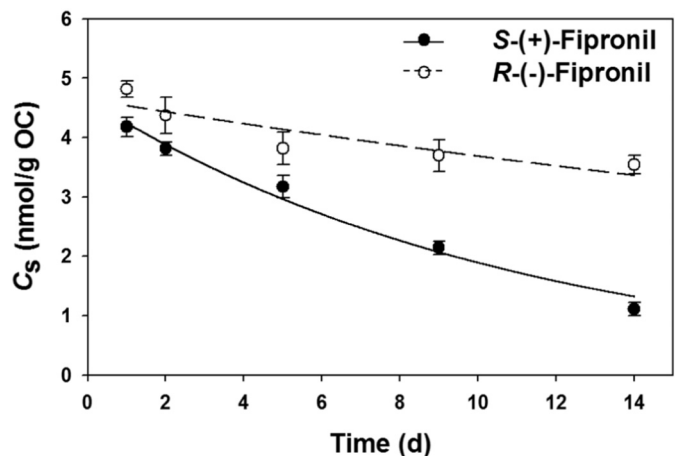


Fig. 2. Stereoselective degradation process of fipronil enantiomers in sediment. Simulative equations for *S*-(+)- and *R*-(-)-fipronil are $C_{S-(+)-fipronil} = 4.64 \times e^{-0.090 \cdot t}$ (solid circle and real line) and $C_{R(-)-fipronil} = 4.64 \times e^{-0.023 \cdot t}$ (hollow circle and dashed line), respectively. Error bars represent standard deviations of three replicates.

3.2. Enantioselective bioaccumulation in *Lumbriculus variegatus*

The overlying water quality was monitored throughout the 28-d bioaccumulation testing including dissolved oxygen (6.5 ± 0.6 mg/L), pH (7.8 ± 0.1), temperature (23.0 ± 0.2 °C), conductivity (356 ± 16 μ S/cm) and ammonia (≤ 0.5 mg/L), and they were all within the acceptable ranges (USEPA, 2000). No mortality or behavioral abnormality was observed for *L. variegatus* after sediment exposure. At the end of uptake phase, the number of blackworms per replicate remained unchanged. The number of organisms slightly increased in the elimination phase, but the increase was not $>20\%$ in any replicates, suggesting reproduction of *L. variegatus* only occurred in the elimination phase (You et al., 2006). Furthermore, wet weight per replicate (146 ± 23 mg) and the lipid content of the blackworms ($1.03 \pm 0.12\%$) were similar among all treatments and the control.

The concentrations of fipronil enantiomers in *L. variegatus* at sampling time intervals during bioaccumulation testing are shown in Table S3. When the blackworms were exposed to fipronil-spiked sediment, body residues of both enantiomers sharply increased with increasing time and reached an apex at 5 d, being 0.975 ± 0.030 and 1.45 ± 0.06 nmol/g lipid for S-(+)- and R(-)-fipronil, respectively. After that, organism concentrations gradually declined until the end of uptake phase. Stereoselective bioaccumulation occurred. At the end of uptake phase, body residues of S-(+)- and R(-)-fipronil were significantly different ($p < 0.05$), being 0.294 ± 0.012 and 0.773 ± 0.039 nmol/g lipid, respectively. Elimination of fipronil in *L. variegatus* was investigated by transferring the organisms to clean sediments after 14-d uptake phase. During elimination phase, the concentrations of both enantiomers descended quickly and approached to 0.0271 ± 0.0040 and 0.0373 ± 0.0060 nmol/g lipid for S-(+)- and R(-)-enantiomer, respectively, at the end of the 28-d bioaccumulation testing.

As shown in Table S3, fipronil selectively accumulated in *L. variegatus* with a preference for R(-)- to S-(+)-enantiomer. The concentration of R(-)-fipronil in organism was approximately 1.5 times higher than that of S-(+)-fipronil at 5 d and 3 times at 14 d. Similar to the reducing trend of EF in sediment, EF values of fipronil in organism continuously decreased over time in the uptake phase (Fig. 1), from 0.435 ± 0.004 at 1 d to 0.274 ± 0.003 at 14 d.

Enantioselective bioaccumulation has been previously reported for other annelids. Liu et al. (2012) reported the concentrations of fipronil enantiomers in *T. tubifex* were significantly different and EF values declined during the 14-d tests regardless of water or soil exposures. Qu et al. (2016b) reported an n-shaped accumulation profile for fipronil enantiomers when studying long-term exposure of fipronil to *A. woodianus*. The trend was similar to that in the present study, but the time to reach the maximum concentrations in biota was species-specific, with *A. woodianus* at 16 d (Qu et al., 2016b) and *L. variegatus* at 5 d (the present study). After reaching the peak concentration, a significant reduction of fipronil residues in *A. woodianus* was noted and the concentrations of fipronil enantiomers were only about 20% at the end of exposure compared with the maximum concentrations at 16 d (Qu et al., 2016b).

As shown in Fig. 1, R(-)-fipronil was the dominating enantiomer in both sediment and organism and EF values continued dropping over the uptake phase. Comparatively, the drop of EF in biota was slower than that in sediment. The difference of EF values between 1 and 14 d was 0.161 ± 0.005 in *L. variegatus* and 0.223 ± 0.012 in sediment. The slopes of EF versus time were not parallel for fipronil in sediment and organism, suggesting enantiomer-specific degradation in sediment was not the only factor influencing enantioselective accumulation of fipronil to *L. variegatus*. Therefore, it is imperative to mechanistically understand the enantioselective TK process of fipronil in biota. The reductive and oxidized metabolites (fipronil sulfide and fipronil sulfone, respectively) are not chiral compounds, thus it was difficult to distinguish whether the metabolites were transformed from S-(+)- or R(-)-fipronil in biota. Instead, TK modeling helps quantitatively understanding the ADME processes and identifying key parameters affecting enantioselective bioaccumulation.

3.3. Toxicokinetic modeling

Changing concentrations of fipronil enantiomers in *L. variegatus* over time were simulated with TK modeling and rate coefficients were attained by fitting the data in uptake and elimination phases simultaneously (Fig. 3 and Table 1). Degradation kinetic model (Eq. (1)) was incorporated into the TK simulation (Eq. (3)) as the degradation of fipronil in sediment significantly affected chemical uptake to the blackworms.

The concentrations of both S-(+)- and R(-)-fipronil in *L. variegatus* started to decline after reaching the peak concentrations at 5 d although the organisms were still exposed to fipronil in sediment (Fig. 3). A similar reduction of tissue concentrations of fipronil in sediment bioaccumulation tests was also reported for *A. woodianus* and *Misgurnus anguillicaudatus* (Qu et al., 2016a, 2018). On the contrary, several studies on the bioaccumulation of fipronil from water to various organisms showed that tissue concentrations reached the steady state after a quick increase at the beginning of exposure (Ashauer et al., 2012; Li et al., 2018; Rosch et al., 2016). Compared with constant fipronil concentrations in water in previous studies, the concentrations of fipronil in sediment significantly declined in the present study as a result of degradation in sediment. Therefore, uptake flux of sediment-bound fipronil to the blackworms decreased over time, causing reduced tissue concentrations. On the other hand, the two lines describing EF trends in sediment and biota intersected (Fig. 1), which indicated that sediment degradation was not the sole reason for decreasing body residues.

Metabolic clearance was another plausible explanation for the decrease of fipronil in organism. For ease of excretion, xenobiotics in biota tended to conjugate with polar compounds including carbohydrates, glutathione and sulfate and the phase II metabolism might become prominent with prolonged exposure time (Katagi, 2010). Induction of phase II enzyme-mediated metabolic clearance would interrupt the steady state of chemicals in organism and phase II metabolism has been previously observed in invertebrates (Ashauer et al., 2012; Scharf et al., 2000). A unified biotransformation rate constant was generally used for short-term exposure in TK model, yet it might fail for biotransformation data simulation in long-term exposure (Manevski et al., 2015). The metabolic clearance process was governed by the activity of metabolic enzymes, which varied with exposure time and chemical concentrations (Katagi, 2010; Stefani Margarido et al., 2013). Therefore, a non-linear Michaelis-Menten model was applied in simulating the metabolic clearance of fipronil enantiomers in TK modeling.

As shown in Table 1, coefficients of determination (COD) for the models regarding to S-(+)- and R(-)-fipronil were 0.991 and 0.925, showing good fitting of experimental data to the TK model with the inclusions of sediment degradation and Michaelis-Menten model. While

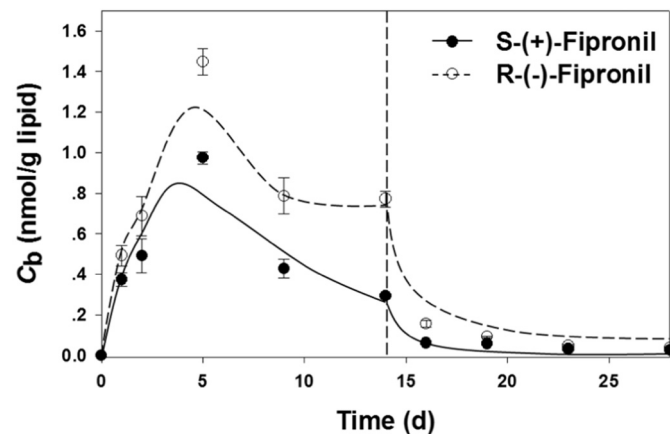


Fig. 3. Toxicokinetic process of fipronil enantiomers in *Lumbriculus variegatus*. Real and dashed lines are simulative curves for S-(+)-fipronil and R(-)-fipronil, respectively. Error bars represent standard deviations of three replicates.

Table 1

Uptake and elimination rate constants (k_u and k_{ep} , respectively) and metabolic parameters (the apparent maximum reaction rate (V_m) and the apparent half-saturation constant (K_s)) estimated from the toxicokinetic model for the bioaccumulation of sediment-associated fipronil enantiomers to *Lumbriculus variegatus*. Coefficients of determination (COD) for the models are also presented.

Enantiomer	k_u (g OC/g lipid/d)	k_{ep} (1/d)	V_m (nmol/g lipid/d)	K_s (nmol/g lipid)	COD
S-(+)-Fipronil	0.121 ± 0.026	0.013 ± 0.009	0.772 ± 0.184	0.789 ± 0.347	0.991
R-(−)-Fipronil	0.714 ± 0.432	0.064 ± 0.059	2.96 ± 1.88	0.159 ± 0.067	0.925

S-(+)-fipronil degraded faster than R-(−)-fipronil in sediment, the later had much higher uptake and elimination rate coefficients (k_u and k_{ep}) in *L. variegatus*, with k_u of 0.714 ± 0.432 and 0.121 ± 0.026 g OC/g lipid/d, and k_{ep} of 0.0636 ± 0.0592 and 0.0130 ± 0.0091/d for R-(−)- and S-(+)-enantiomer, respectively. The R-(−)-fipronil had a greater apparent maximum reaction rate (V_m , 2.96 ± 1.88 nmol/g lipid/d) than that of S-(+)-fipronil (0.772 ± 0.184 nmol/g lipid/d), but a smaller apparent half-saturation constant (K_s). Similarly, Lin et al. (2016) found the V_m of R-(+)-flufiprole was nearly 3-fold compared with S-(−)-flufiprole in rat liver microsomes. As a consequence of enantioselective ADME process in *L. variegatus*, R-(−)-fipronil was preferentially accumulated from sediment to organism.

For better assessing the contribution of individual ADME processes in enantioselective bioaccumulation of fipronil, the integrated fluxes of absorption, metabolism and elimination processes over 14 d were calculated. The integrated absorption fluxes within 14 d were 4.49 and 39.7 nmol/g lipid for S-(+)- and R-(−)-fipronil, respectively. Significantly greater absorption of R-(−)- than S-(+)-enantiomer was also noted for the bioaccumulation of tebuconazole and alpha-cypermethrin in soil by *E. fetida* (Diao et al., 2011; Yu et al., 2012). The integrated metabolism fluxes within the 14-d uptake were 4.09 and 34.1 nmol/g lipid for S-(+)- and R-(−)-fipronil, respectively. To have a higher value of V_m and a smaller K_s , R-(−)-fipronil was metabolized more easily than S-(+)-fipronil in the blackworms. This was in accordance with a previous study by Qu et al. (2016a) who reported that R-(−)-fipronil in *A. woodiana* was metabolized more rapidly than S-(+)-fipronil. The integrated elimination fluxes within 14 d were similar for S-(+)- and R-(−)-fipronil (0.0938 and 0.111 nmol/g lipid, respectively). It is expected that both enantiomers had similar elimination flux. *L. variegatus* has a large surface area to volume ratio and intensive blood circulation in the skin, thus the elimination of a chemical was mainly controlled by the physiological characteristic of the organisms rather than chemical properties (Zhang et al., 2013).

Overall, TK modeling quantitatively explained the observed preferential accumulation of R-(−)-fipronil from sediment to *L. variegatus*. Higher uptake rate coefficient and greater concentration of R-(−)-fipronil in sediment due to faster degradation of sediment-associated S-(+)-fipronil were the main reasons for greater concentrations of R-(−)-fipronil in the blackworms. On the contrary, faster biotransformation of R-(−)-fipronil might reduce its tissue concentrations, but biotransformation had less impact on the enantioselective bioaccumulation compared with absorption. The contradictory effects of enantioselective absorption and biotransformation on fipronil bioaccumulation explained slower decline of EF in tissue over time than that in sediment. While k_{ep} values were different for the two enantiomers, elimination flux showed little chiral difference. Katagi and Ose (2015) also found that the difference of uptake and degradation rates were likely the controlling factors of enantioselectivity in bioaccumulation of pesticides by the earthworms.

4. Conclusions

Enantioselective bioaccumulation of sediment-bound fipronil to *L. variegatus* was analyzed, and the concentrations of R-(−)-fipronil were found significantly higher than S-(+)-fipronil in both sediment and *L. variegatus*. Toxicokinetic parameters simulated from the newly constructed TK model with inclusions of sediment degradation and

Michaelis-Menten biotransformation models helped to mechanistically understand the enantioselective bioaccumulation process.

Faster degradation of S-(+)-fipronil was the reason for higher concentrations of R-(−)-fipronil in sediment. Preferential absorption of R-(−)-fipronil from sediment to the blackworms was the main reasons for higher tissue concentrations of R-(−)-fipronil. In addition, the biotransformation of R-(−)-fipronil was faster than S-(+)-fipronil, but it played less role enantioselective bioaccumulation compared with uptake process. The present study showed TK modeling could serve as a great tool for quantitatively understanding the enantioselective bioaccumulation of chiral chemicals in organism, which would significantly affect the toxicity and risk of the chemical.

Acknowledgements

This work was supported by the National Science Foundation of China (41773101 and 41473106), Department of Science and Technology of Guangdong Province (2015A030310219, 2017A020216002 and 2017A030313065) and Jinan University (21617452). This is contribution No. IS-2676 from GIGCAS.

Conflict of interest

The authors have no conflicts of interest.

Appendix A. Supplementary data

Supplementary data to this article can be found online at <https://doi.org/10.1016/j.scitotenv.2019.03.490>.

References

- Ashauer, R., Escher, B.I., 2010. Advantages of toxicokinetic and toxicodynamic modeling in aquatic ecotoxicology and risk assessment. *J. Environ. Monit.* 12, 2056–2061.
- Ashauer, R., Jager, T., 2018. Physiological modes of action across species and toxicants: the key to predictive ecotoxicology. *Environ. Sci.: Processes Impacts* 20, 48–57.
- Ashauer, R., Hintermeister, A., O'Connor, I., Elumelu, M., Hollender, J., Escher, B.I., 2012. Significance of xenobiotic metabolism for bioaccumulation kinetics of organic chemicals in *Gammarus pulex*. *Environ. Sci. Technol.* 46, 3498–3508.
- Brennan, A.A., You, J., Lydy, M.J., 2009. Comparison of cleanup methods for fipronil and its degradation products in sediment extracts. *Talanta* 78, 1408–1413.
- Cantillana, T., 2009. Toxicologically Important DDT Metabolites Synthesis, Enantioselective Analysis and Kinetics. Department of Environmental Chemistry Stockholm University Stockholm, pp. 22–41.
- Diao, J.L., Xu, P., Liu, D.H., Lu, Y.L., Zhou, Z.Q., 2011. Enantiomer-specific toxicity and bioaccumulation of alpha-cypermethrin to earthworm *Eisenia fetida*. *J. Hazard. Mater.* 192, 1072–1078.
- Ding, Y.P., Landrum, P.F., You, J., Harwood, A.D., Lydy, M.J., 2012. Use of solid phase microextraction to estimate toxicity: relating fiber concentrations to toxicity-part I. *Environ. Toxicol. Chem.* 31, 2159–2167.
- Hegeman, W., Laane, R.W.P.M., 2002. Enantiomeric enrichment of chiral pesticides in the environment. *Rev. Environ. Contam. Toxicol.* 137, 85–116.
- Jones, W.J., Mazur, C.S., Kenneke, J.F., Garrison, A.W., 2007. Enantioselective microbial transformation of the phenylpyrazole insecticide fipronil in anoxic sediments. *Environ. Sci. Technol.* 41, 8301–8307.
- Katagi, T., 2010. Bioconcentration, bioaccumulation, and metabolism of pesticides in aquatic organisms. *Rev. Environ. Contam. Toxicol.* 204, 1–132.
- Katagi, T., Ose, K., 2015. Toxicity, bioaccumulation and metabolism of pesticides in the earthworm. *J. Pestic. Sci.* 40, 69–81.
- Konwick, B.J., Garrison, A.W., Black, M.C., Avants, J.K., Fisk, A.T., 2006. Bioaccumulation, biotransformation, and metabolite formation of fipronil and chiral legacy pesticides in rainbow trout. *Environ. Sci. Technol.* 40, 2930–2936.
- Kumar, N., Mukherjee, I., Sarkar, B., Paul, R.K., 2017. Degradation of tricyclazole: effect of moisture, soil type, elevated carbon dioxide and Blue Green Algae (BGA). *J. Hazard. Mater.* 321, 517–527.

- Landrum, P.F., Lee, H., Lydy, M.J., 1992. Toxicokinetics in aquatic systems: model comparisons and use in hazard assessment. *Environ. Toxicol. Chem.* 11, 1709–1725.
- Lewis, D.L., Garrison, A.W., Wommack, K.E., Whittemore, A., Stuedler, P., Melillo, J., 1999. Influence of environmental changes on degradation of chiral pollutants in soils. *Nature* 401, 898–901.
- Li, H.Z., Zhang, B.Z., Wei, Y.L., Wang, F., Lydy, M.J., You, J., 2014. Bioaccumulation of highly hydrophobic organohalogen flame retardants from sediments: application of toxicokinetics and passive sampling techniques. *Environ. Sci. Technol.* 48, 6957–6964.
- Li, H.Z., You, J., Wang, W.X., 2018. Multi-compartmental toxicokinetic modeling of fipronil in tilapia: accumulation, biotransformation and elimination. *J. Hazard. Mater.* 360, 420–427.
- Lin, C.M., Miao, Y.L., Qian, M.R., Wang, Q., Zhang, H., 2016. Enantioselective metabolism of flufenprole in rat and human liver microsomes. *J. Agric. Food Chem.* 64, 2371–2376.
- Liu, W.P., Gan, J.Y., Schlenk, D., Jury, W.A., 2005. Enantioselectivity in environmental safety of current chiral insecticides. *PNAS* 102, 701–706.
- Liu, T.T., Wang, P., Lu, Y.L., Zhou, G.X., Diao, J.L., Zhou, Z.Q., 2012. Enantioselective bioaccumulation of soil-associated fipronil enantiomers in *Tubifex tubifex*. *J. Hazard. Mater.* 219–220, 50–56.
- Manevski, N., Swart, P., Balavenkatraman, K.K., Bertschi, B., Camenisch, G., Kretz, O., Schiller, H., Walles, M., Ling, B., Wettstein, R., Schaefer, D.J., Itin, P., Ashton-Chess, J., Pognan, F., Wolf, A., Litherland, K., 2015. Phase II metabolism in human skin: skin explants show full coverage for glucuronidation, sulfation, N-acetylation, catechol methylation, and glutathione conjugation. *Drug Metab. Dispos.* 43, 126–139.
- Mehler, W.T., You, J., Keough, M.J., Lydy, M.J., Pettigrove, V., 2018. Improvements and cost-effective measures to the automated intermittent water renewal system for toxicity testing with sediments. *Ecotoxicol. Environ. Saf.* 151, 62–67.
- Nillos, M.G., Lin, K.D., Gan, J., Bondarenko, S., Schlenk, D., 2009. Enantioselectivity in fipronil aquatic toxicity and degradation. *Environ. Toxicol. Chem.* 28, 1825–1833.
- Qian, Y., Wang, C., Wang, J.H., Zhang, X.F., Zhou, Z.Q., Zhao, M.R., Lu, C.S., 2017. Fipronil-induced enantioselective developmental toxicity to zebrafish embryo-larvae involves changes in DNA methylation. *Sci. Rep.* 7, 1–11.
- Qin, F., Gao, Y.X., Xu, P., Guo, B.Y., Li, J.Z., Wang, H.L., 2015. Enantioselective bioaccumulation and toxic effects of fipronil in the earthworm *Eisenia foetida* following soil exposure. *Pest Manag. Sci.* 71, 553–561.
- Qu, H., Wang, P., Ma, R.X., Qiu, X.X., Xu, P., Zhou, Z.Q., Liu, D.H., 2014. Enantioselective toxicity, bioaccumulation and degradation of the chiral insecticide fipronil in earthworms (*Eisenia foetida*). *Sci. Total Environ.* 485–486, 415–420.
- Qu, H., Ma, R.X., Liu, D.H., Gao, J., Wang, F., Zhou, Z.Q., Wang, P., 2016a. Environmental behavior of the chiral insecticide fipronil: enantioselective toxicity, distribution and transformation in aquatic ecosystem. *Water Res.* 105, 138–146.
- Qu, H., Ma, R.X., Liu, D.H., Jing, X., Wang, F., Zhou, Z.Q., Wang, P., 2016b. The toxicity, bioaccumulation, elimination, conversion of the enantiomers of fipronil in *Anodonta woodiana*. *J. Hazard. Mater.* 312, 169–174.
- Qu, H., Ma, R.X., Wang, F., Gao, J., Wang, P., Zhou, Z.Q., Liu, D.H., 2018. The effect of biochar on the mitigation of the chiral insecticide fipronil and its metabolites burden on loach (*Misgurnus anguillicaudatus*). *J. Hazard. Mater.* 360, 214–222.
- Rosch, A., Anliker, S., Hollender, J., 2016. How biotransformation influences toxicokinetics of azole fungicides in the aquatic invertebrate *Gammarus pulex*. *Environ. Sci. Technol.* 50, 7175–7188.
- Scharf, M.E., Siegfried, B.D., Meinke, L.J., Chandler, L.D., 2000. Fipronil metabolism, oxidative sulfone formation and toxicity among organophosphate- and carbamate-resistant and susceptible western corn rootworm populations. *Pest Manag. Sci.* 56, 757–766.
- Stefani Margarido, T.C., Felicio, A.A., de CerqueiraRossa-Feres, D., de Almeida, E.A., 2013. Biochemical biomarkers in *Scinax fuscovarius* tadpoles exposed to a commercial formulation of the pesticide fipronil. *Mar. Environ. Res.* 91, 61–67.
- Tan, H.H., Cao, Y.S., Tang, T., Qian, K., Chen, W.L., Li, J.Q., 2008. Biodegradation and chiral stability of fipronil in aerobic and flooded paddy soils. *Sci. Total Environ.* 407, 428–437.
- US Environmental Protection Agency, 2000. Methods for measuring the toxicity and bioaccumulation of sediment-associated contaminants with freshwater invertebrates. EPA 600/R-99/064 (Washington, DC).
- Wei, Y.L., Li, H.Z., Zhang, J.J., Xiong, J.J., Yi, X.Y., You, J., 2017. Legacy and current-use insecticides in agricultural sediments from south China: impact of application pattern on occurrence and risk. *J. Agric. Food Chem.* 65, 4247–4254.
- Weston, D.P., Lydy, M.J., 2014. Toxicity of the insecticide fipronil and its degradates to benthic macroinvertebrates of urban streams. *Environ. Sci. Technol.* 48, 1290–1297.
- Wiberg-Larsen, P., Graeber, D., Kristensen, E.A., Baatrup-Pedersen, A., Friberg, N., Rasmussen, J.J., 2016. Trait characteristics determine pyrethroid sensitivity in non-standard test species of freshwater macroinvertebrates: a reality check. *Environ. Sci. Technol.* 50, 4971–4978.
- Xu, C.Y., Lin, X.M., Yin, S.S., Zhao, L., Liu, Y.X., Liu, K., Li, F., Yang, F.X., Liu, W.P., 2018. Enantioselectivity in biotransformation and bioaccumulation processes of typical chiral contaminants. *Environ. Pollut.* 243, 1274–1286.
- You, J., Landrum, P.F., Lydy, M.J., 2006. Comparison of chemical approaches for assessing bioavailability of sediment-associated contaminants. *Environ. Sci. Technol.* 40, 6348–6353.
- Yu, D.Y., Li, J.Z., Zhang, Y.F., Wang, H.L., Guo, B.Y., Zheng, L., 2012. Enantioselective bioaccumulation of tebuconazole in earthworm *Eisenia foetida*. *J. Environ. Sci.* 24, 2198–2204.
- Zhang, B.Z., Li, H.Z., Wei, Y.L., You, J., 2013. Bioaccumulation kinetics of polybrominated diphenyl ethers and decabromodiphenyl ethane from field-collected sediment in the oligochaete, *Lumbriculus variegatus*. *Environ. Toxicol. Chem.* 32, 2711–2718.